Neutron stars with variable internal heaters

E. A. Chaikin[1,2], A. A. Kaurov[3], A. D. Kaminker[1] and D. G. Yakovlev[1]

[1] *Ioffe Institute, Politechnicheskaya 26, 194021, St. Petersburg, Russia*
[2] *Peter the Great St. Petersburg Polytechnic University, Politechnicheskaya 26, 194021, St. Petersburg, Russia*
[3] *Department of Astronomy & Astrophysics. University of Chicago, IL 60637 USA*

PACS 97.60.Jd – Neutron stars
PACS 65.90.+i – Other topics in thermal properties of condensed matter
PACS 44.40.+a – Thermal radiation

Abstract – We study thermal radiation of a warm neutron star with a variable shell-like heater located in its crust. The heater and the star are taken to be initially in a stationary state. Then we increase or decrease the heat power for some period of time which produces a peak or a dip of the thermal surface emission; afterwards the stationary state is restored. Only a small fraction of the generated heat is thermally emitted through the surface. Time variation of the surface luminosity is weakened and distorted with respect to the variation of the generated heat power; the former variation can be observable only under special conditions – neutron stars are "hiding" internal temperature variations. These results can be useful for interpretation of observations of neutron stars with variable thermal surface emission, particularly, magnetars and transiently accreting neutron stars in low-mass X-ray binaries.

Introduction. – Internal structure of neutron stars (most compact stars containing superdense matter with poorly known properties) is a long-standing fundamental astrophysical and physical problem [1, 2]. There is solid observational evidence that some neutron stars possess internal heat sources which may have different nature [3–5]. These internal heaters can strongly affect the evolution of neutron stars, so that their studies are of primary importance.

Here we investigate such sources located in a neutron star crust, which is a thin layer under the surface (about 1% of star's mass); it surrounds superdense, massive and bulky stellar core [1]. To be general, we do not specify the nature of the heater. We use a neutron star cooling code and calculate the (observable) thermal emission from the surface. Our main aim is to analyze possible signatures of the heater in the surface emission and the conditions under which this emission can be observed; it is also important to know what information on the heater can be inferred from such observations.

Previously, we have investigated (quasi-)stationary heaters [6, 7] and have shown that the strongest effects on the thermal surface emission are produced by the heaters located in the outer star's crust, sufficiently close to the surface. Otherwise the generated heat is mainly conducted to the core and radiated away by neutrinos.

Here we study a variable heater which increases or decreases its power for some period of time and produces a peak or a dip in the thermal surface emission. Under which conditions are these variations observable? A similar problem has been studied for short (a few hours) and strong heater's energy generations [8]. We extend these studies for longer heater's variations (see below) and present the first results.

Simulations. – For simulations, we have used our new one-dimensional cooling code which calculates the evolution of the temperature in a spherically symmetric star with a nucleon core. The code is written in Python programming language. It adopts a one-dimensional mesh with 350 radial spherical cells, from the star's center to the density $\rho_b = 10^9$ g cm^{-3}. The code is based on the implicit Euler backward method which makes simulations stable under a vast range of initial conditions. It solves for the temperature distribution $T(\rho, t)$ within the star at densities $\rho > \rho_b$, taking into account thermal conduction, neutrino cooling and an assumed heating. General Relativity effects are included exactly. Microphysics input is mainly the same as in our standard one-dimensional cooling code [9]. In particular, the effects of neutron and proton superfluidities on the neutrino emissivity and heat capacity of the matter are included in the same manner. However, for simplicity, we will neglect these effects here because our heater is sufficiently close to the surface where the effects of superfluidity on heat transport are rather unimportant.

The effective surface temperature of the star T_s is connected to the temperature T_b at $\rho = \rho_b$ through a special $T_s - T_b$ relation which is calculated separately using a quasi-stationary

plane-parallel approximation [10]. We have employed a recently calculated relation [11] for the surface layers made of iron. For surface temperatures $T_s \gtrsim 1$ MK of our interest, typical heat propagation time from $\rho_b = 10^9$ g cm^{-3} through this heat blanketing envelope is $t_{th} \sim 1$ d. Therefore, our code allows us to study surface temperature variations no shorter than about 1 d. If we took a standard model of the heat-blanketing envelope with $\rho_b = 10^{10}$ g cm^{-3}, the "time resolution" of our code would be $t_{th} \sim 1$ yr.

For simulations, we have chosen one neutron star model, with the BSk21 equation of state [12] of nucleon matter in the core. The gravitational mass of the chosen model is $M = 1.4\,M_\odot$ and the circumferential radius $R = 12.6$ km. We have approximated the heater by a thin spherical layer ($\rho_1 \le \rho \le \rho_2$). The heat power $Q(\rho, t)$ [erg cm^{-3} s^{-1}] has been taken zero outside this layer and independent of ρ within it. Within the heater, we have assumed the relationship

$$Q(\rho, t) = H_c + H_{var}(t), \tag{1}$$

where H_c is a constant stationary heat power, and $H_{var}(t)$ is a variation given by

$$H_{var}(t) = H_0 \sin^2(\pi t/\Delta t) \quad \text{at } 0 \le t \le \Delta t, \tag{2}$$

with $H_{var}(t) = 0$ otherwise. Here we assume that the generated heat starts to vary at some moment of time $t = 0$ and ends to vary at $t = \Delta t$. Thus, H_0 is a variation amplitude and Δt is a variation duration. The time-integrated heat production of variable energy per cm^3 in the heater is

$$\Delta E_{var} = \int_0^{\Delta t} H_{var}(t)\,\mathrm{d}t = \frac{1}{2}\,H_0\,\Delta t. \tag{3}$$

If $H_0 > 0$ we create a heat peak, otherwise ($H_0 < 0$) a heat dip. The previous consideration of Pons and Rea [8] formally corresponds to an instantaneous (delta function) energy release, $H_{var}(t) = \Delta E_{var}\,\delta(t)$.

We have used the cooling code to follow the evolution of the star. At the first stage we evolve the star with the constant heat power H_c in the heater. Initially the star cools down but then it reaches a stationary state stabilized by the constant heating [6]; in this state the star is non-isothermal inside, the maximum temperature $T = T_h$ is reached in the heater. Then at some moment of time (to be denoted as $t = 0$) we vary the heat power in accordance with (2). In response, the surface emission starts to vary but finally the heat variation stops and the star returns to its initial stationary state. We have calculated the total heat generation power $L_h^\infty(t)$ [erg s^{-1}] and the total surface luminosity $L_s^\infty(t)$, both redshifted for a distant observer.

We have mainly considered two positions of the heater. In the first case (of the so called "outer heater") we assume $\rho_1 = 10^{11}$ g cm^{-3} and $\rho_2 = 10^{12}$ g cm^{-3}. In the second case (of the "inner heater") we take $\rho_1 = 10^{12}$ g cm^{-3} and $\rho_2 = 1.27 \times 10^{13}$ g cm^{-3}; the value of ρ_2 is chosen in such a way to have equal $L_h^\infty(t)$ at the same H_c, H_0 and Δt for both heaters. In simulations, we have varied H_c, H_0 and Δt. For heat peaks, we have taken $H_0 = 9\,H_c$, while for dips $H_0 = -H_c$. In the latter case the heater becomes entirely switched off, $Q(t) = 0$, at $t = \frac{1}{2}\,\Delta t$. Therefore, we have considered very pronounced variations. The reason for that will be clarified below.

Results. – We have performed a number of cooling calculations and present typical results.

Figs. 1 and 2 compare the generated heat power $L_h^\infty(t)$ with the thermal surface luminosity $L_s(t)$ of the star. Fig. 1 corresponds to heat peaks, whereas Fig. 2 to heat dips. Three panels on each figure, 1A–1C and 2A–2C, refer to three stationary heat intensities, $H_c = 5{\times}10^{17}$, $5{\times}10^{18}$ and $5{\times}10^{19}$ erg cm^{-3} s^{-1}, respectively (to progressively stronger stationary heater and overall warmer star). The upper curves on each figure show $L_h^\infty(t)$ while the low curves present $L_s^\infty(t)$. Each panel displays the results for the two positions of the heater. For both positions, the heat powers $L_h^\infty(t)$ (at the same H_0 and Δt) are equal and merge in single curves. The surface luminosities $L_s^\infty(t)$ are naturally different; the deeper the heater, the lower $L_s^\infty(t)$ (the smaller fraction of heat reaches the surface). Each figure presents the results for three durations of heater's variability, Δt= 1, 10, and 100 years.

Fig. 1 displays the variability of $L_h^\infty(t)$ and $L_s^\infty(t)$ under energy releases at $H_0 = 9\,H_c$. In response to the energy release, the surface emission increases, reaches maximum and then decreases to its initial pre-burst level. Filled dots show maxima of $L_h^\infty(t)$ (assumed to be at $t = \frac{1}{2}\Delta t$) and of $L_s^\infty(t)$. One can see that in any case only a small fraction of the generated heat is emitted from the stellar surface ($L_s^\infty \ll L_h^\infty$). The behavior of the surface radiation is seen to be drastically dependent of the energy release duration Δt and amplitude H_0, as well as of the pre-burst heater's amplitude H_c (i.e. on the thermal state of the star before the burst). It is convenient to introduce characteristic heat diffusion time scale t_{diff} from the heater to the surface, characteristic time scale Δt_s for variability of the surface emission, and typical heater's temperature $T \approx T_h$. These quantities depend on the heater's parameters. Typically, $t_{diff} \sim$ a few years for the outer heater and several times larger for the inner heater; the warmer the star the larger t_{diff}.

Consider, for instance, Fig. 1A which is plotted for a relatively low $H_c = 5 \times 10^{17}$ erg cm^{-3} s^{-1}. For the shortest energy release (Δt=1 yr, solid lines), the variation of the thermal surface emission is nearly invisible (not detectable). The reason is twofold. First, the total amount of the released energy is not large (even if the amplitude H_0 is pretty high). Second, the heat propagation time t_{diff} is longer than the energy release duration Δt (so that the surface variability lasts for $\Delta t_s \sim t_{diff} \gg \Delta t$). This disperses $L_s^\infty(t)$ over the long time interval Δt_s, decreasing the peak of the surface emission. The peak shape of $L_s^\infty(t)$ (almost invisible for the scales in Fig. 1A) contains a rapid surface luminosity rise (t_{diff} in a pre-burst star) and a slower luminosity decay (t_{diff} in a star heated by the energy release).

For the 10-year long energy release (dashed lines) in Fig. 1A, the increase of the surface thermal emission is already quite visible. The surface luminosity profiles $L_s^\infty(t)$ (lower curves) have a pronounced peak shape. The peak profiles significantly differ from the profile of the heater's power $L_h^\infty(t)$ (the upper curve). Specifically, the peaks of $L_s^\infty(t)$ are smaller, broader,

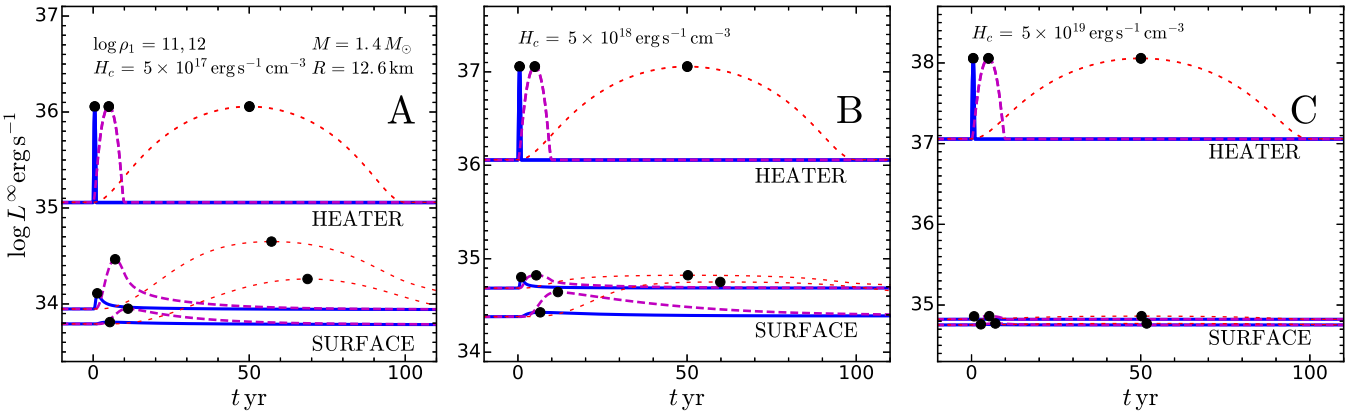

Fig. 1: (Colour online) The heater's power $L_{\rm h}^{\infty}(t)$ (upper curves) and surface luminosity $L_{\rm s}^{\infty}(t)$ (lower curves) of the star versus time t for heater's energy release which start at $t = 0$. Three panels A, B, and C, correspond to three stationary heat intensities, $H_{\rm c} = 5\times10^{17}$, 5×10^{18} and 5×10^{19} erg cm^{-3} s^{-1}, respectively. The energy generation amplitudes are taken to be $H_0 = 9\,H_{\rm c}$. Solid, dashed, and dotted lines refer to the three energy release durations, $\Delta t = 1, 10$ and 100 yr, respectively. The heater is placed either closer to the surface ($\rho_1 = 10^{11}$ g cm^{-3}) or deeper in the crust ($\rho_1 = 10^{12}$ g cm^{-3}). The heat power is independent of ρ_1 (leading to one $L_{\rm h}^{\infty}(t)$ curve for two values of ρ_1), while $L_{\rm s}^{\infty}(t)$ decreases with the depth of the heater (lower $L_{\rm s}^{\infty}(t)$ for higher ρ_1). Filled dots indicate maxima of $L_{\rm s}^{\infty}(t)$ and $L_{\rm h}^{\infty}(t)$. See text for details.

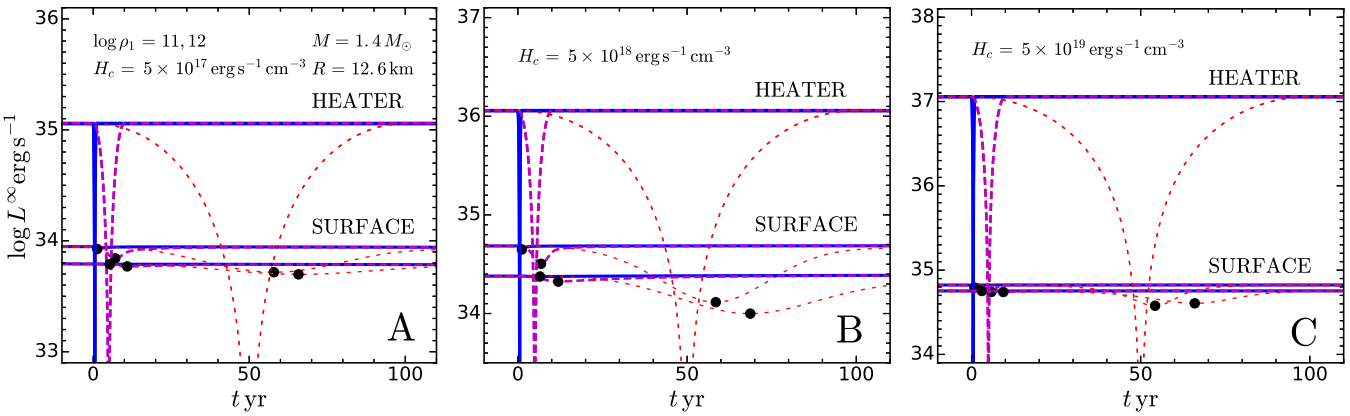

Fig. 2: (Colour online) Same as in Fig. 1 but for heat dips down to zero heat intensity at $t = \Delta t/2$; $H_0 = -H_{\rm c}$. Filled dots indicate minima of $L_{\rm s}^{\infty}(t)$. See text for details.

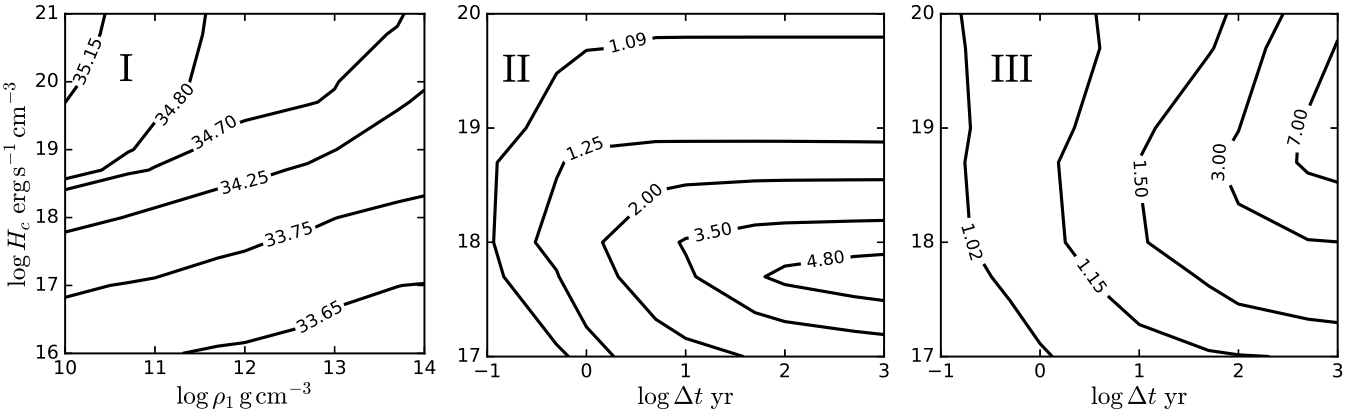

Fig. 3: Panel I: Lines of constant $\log L_{\rm s}^{\infty}$ [erg s^{-1}] (numbers next to the curves) versus ρ_1 and $H_{\rm c}$ for stationary heaters which have the same $L_{\rm h}^{\infty}$ for any ρ_1 at a fixed $H_{\rm c}$. Other panels: Lines of constant ratios (numbers next to the curves) of $L_{\rm max}^{\infty}/L_{\rm c}^{\infty}$ (panel II, heat releases, $H_0 = 9\,H_{\rm c}$, as in Fig. 1) and of $L_{\rm c}^{\infty}/L_{\rm min}^{\infty}$ (panel III, heat dips, $H_0 = -H_{\rm c}$, as in Fig. 2) versus Δt and $H_{\rm c}$; $L_{\rm c}^{\infty} = L_{\rm s}^{\infty}$ is the thermal surface luminosity of the star prior to heater's variations; $L_{\rm max}^{\infty}$ is the maximum surface luminosity for peaks (filled dots in Fig. 1), and $L_{\rm min}^{\infty}$ is the minimum surface luminosity for dips (filled dots in Fig. 2).

and asymmetrical, whereas the peak of $L_h^\infty(t)$ is symmetric with respect to $t = \frac{1}{2}\Delta t$. In addition, the peaks of $L_s^\infty(t)$ essentially depend on the heater's position. The peak shifts are naturally explained by a finite diffusion time $t_{\rm diff}$. In our particular case, the peak shift for the outer heater is about 2 years, while the shift for the inner heater is about 7 years.

For the longest energy release displayed in Fig. 1A ($\Delta t = 100$ yr, dotted lines) the situation is basically the same but better visible in the figure. The $L_s^\infty(t)$ peaks are damped, shifted and broadened with respect to the $L_h^\infty(t)$ peak. The $L_s^\infty(t)$ peak maximum for the outer heater is only 50% higher than the analogous maximum for the shorter energy release, $\Delta t = 10$ yr. This is because in both cases, $\Delta t = 10$ and 100 yrs, the characteristic heat diffusion time $t_{\rm diff}$ is shorter than Δt (so that now $\Delta t_s \sim \Delta t$). Therefore, very roughly, the situation is quasi-stationary; the heater's power varies slowly and the thermal emission approximately follows these variations. With the growth of Δt the peak shape becomes progressively more symmetric, resembling the shape of $L_h^\infty(t)$. Nevertheless, the $L_s^\infty(t)$ peak maximum for the inner heater at $\Delta t = 100$ yrs is much higher than the corresponding maximum at $\Delta t = 10$ yr. Now the longer energy release is roughly quasi-stationary, while the shorter one is not.

Even longer energy releases, with $\Delta t \gtrsim 100$ yrs, would be more quasi-stationary. However, such very long energy releases would be not detectable (an observer would consider such sources as not variable). Therefore, the most favorable variations to be detected are those from internal energy releases of intermediate duration, with Δt from a few to a few tens yrs. Another important condition concerns the variation amplitude H_0 of the heat generation. In Fig. 1 we have assumed rather strong variations, $H_0 = 9\,H_c$. Had we taken lower H_0, the variations of $L_s^\infty(t)$ would be even weaker.

Fig. 1B shows basically the same quantities as Fig. 1A but for a 10 times stronger stationary heater ($H_c = 5 \times 10^{18}$ erg cm^{-3} s^{-1}), taking again $H_0 = 9\,H_c$. Then the star is overall warmer. All the effects mentioned above (suppression, shift and broadening of $L_s^\infty(t)$ peaks with respect to $L_h^\infty(t)$ ones) are naturally available here but they are quantitatively different, and the fraction of the heat radiated through the surface is lower (the latter conclusion coincides with that made for stationary heaters [7]). As in Fig. 1A, the variability of $L_s^\infty(t)$ for the short-term heater, $\Delta t = 1$ yr, is almost invisible. Moreover, the variations of $L_s^\infty(t)$ for the inner heater become almost invisible for any Δt. This is because the thermal conductivity in the warmer star is lower and the heat diffusion to the surface slower. Nevertheless, the variations of $L_s^\infty(t)$ for the outer heater at $\Delta t = 10$ and 100 yrs remain quite noticeable.

Finally, Fig. 1C shows the same curves as in Figs. 1A and 1B, but for much warmer star, with $H_c = 5 \times 10^{19}$ erg cm^{-3} s^{-1}. As shown in [6–8], this case is special because the temperature in the heater becomes so high ($T_h \gtrsim 10^9$ K) that the neutrino cooling in the heater is more efficient than the thermal conduction; the generated heat is mostly carried away by neutrinos. The fraction of heat emitted from the surface becomes extremely low. When an extra heat is generated, it is taken away by neutrinos. Accordingly, the surface emission shows almost no time variations for both heater's positions. If we increased H_c and/or H_0 further, this would have nearly no effect on the thermal surface emission owing to the same strong neutrino cooling in the heater. Thus the time variability of the heater in such a warm neutron star will be invisible on the surface.

Based on Figs. 1A–1C we can roughly distinguish three main regimes of surface variability of the star.

1. The regime of dynamic response to an internal rapid energy release ($\Delta t \lesssim t_{\rm diff}$) in a not too hot star ($T_h \lesssim 10^9$ K). Is characterized by a rather rapid rise and longer decay on diffusion time-scales $\Delta t_c \sim t_{\rm diff}$. The peak of the surface emission weakly depends on Δt.

2. The regime of quasi-stationary response in a not too hot star ($T_h \lesssim 10^9$ K) to a slow energy release ($\Delta t \gtrsim t_{\rm diff}$). Produces a peak of the surface emission which resembles the internal energy release, lasts for $\sim \Delta t$, and weakly depends on $t_{\rm diff}$.

3. The regime of efficient neutrino cooling of the heater in a hot star ($T_h \gtrsim 10^9$ K). Leads to almost no variations of the surface emission.

These three regimes are schematic; a real burst can be a combination.

The peak shapes of $L_s^\infty(t)$ in the dynamical regime qualitatively agree with the shapes obtained previously [8] for very short energy releases. Note that Pons and Rea [8] have used a two-dimensional (2D) cooling code and studied a heater in the form of a hot spot or a spherical layer under the stellar surface. In both cases the authors included the effects of strong magnetic fields, which mainly affect heat conduction, while we have not included such effects here.

Figs. 2A–2C are essentially the same as 1A–1C but they are plotted for heater's dips (to zero intensity, $Q = 0$ at $t = \frac{1}{2}\Delta t$; $H_0 = -H_c$) instead of energy releases. These dips are naturally accompanied by the dips of the surface emission. Nevertheless, the surface emission dips not to zero but to finite minimum values shown by filled dots. Such minima are again shifted with respect to the minima of $L_h^\infty(t)$ due to finite heat diffusion time scales. In addition, the dips of $L_s^\infty(t)$ become narrower than the dips of $L_h^\infty(t)$ (while the peaks of $L_s^\infty(t)$ in Fig. 1 became broader than the peaks of $L_h^\infty(t)$). Other effects of $L_h^\infty(t)$ dips on $L_s^\infty(t)$ in Fig. 2 are more or less similar to the effects of $L_h^\infty(t)$ for energy releases in Fig. 1. Note that at $\Delta t = 100$ yrs, the dips of $L_s^\infty(t)$ are stronger. Were the heater's dips weaker (not to zero intensity), the variations of $L_s^\infty(t)$ would be even less pronounced.

Fig. 3.I shows isolines of constant $\log L_s^\infty$ for a stationary (pre-burst) star supported by a steady heater of fixed amplitude H_c (no heater's variations there). The isolines are plotted versus heater's position, $\log \rho_1$ (varied widely over the crust), and amplitude H_c. For each ρ_1 the inner heater's density ρ_2 is chosen in such a way to have equal L_h^∞ at a fixed H_c. The figure summarizes all the information on steady heaters discussed above. In particular, the deeper the heater with fixed L_h^∞ the smaller L_s^∞; and at very large H_c the surface luminosity saturates (stops to depend on H_c).

Figs. 3.II and 3.III summarize our analysis of energy releases (Fig. 1) and dips (Fig. 2). These figures show isolines of ratios α of the maximum to minimum thermal surface luminosity. The values of α are given near the curves. Figs. 3.II and 3.III display α in the $\Delta t - H_0$ plane for the outer heater as an example. If L_s^∞ does not vary at all, then $\alpha = 1$. The larger α, the stronger (better observable) variations. For the energy releases (Fig. 3.II), we take $H_0 = 9\,H_c$ and set $\alpha = L^\infty_{max}/L^\infty_c$, where L^∞_{max} is the maximum surface luminosity (filled dots in Fig. 1) and L^∞_c is the stationary pre-burst surface luminosity. For the dips (Fig. 3.III), we assume $H_0 = -H_c$ and plot $\alpha = L^\infty_c/L^\infty_{min}$, where L^∞_{min} is the minimum surface luminosity (filled dots in Fig. 2). Qualitatively, Figs. 3.II and 3.III are similar and indicate that to obtain noticeable variations of the surface emission (larger α), one needs intermediate heater ($H_c \sim (1-5)\times 10^{18}$ erg cm^{-3} s^{-1}) and sufficiently long variations of the heater ($\Delta t \gtrsim 10$ yrs). A weaker heater would produce weaker variations of the surface emission. A stronger heater will overheat the nearby matter and switch on powerful neutrino cooling of the heater; shorter variations would not produce enough heat to disturb the surface emission. In addition, too slow variations of the surface emission ($\Delta t \gg 10$ yrs), even if they are large, would be difficult to detect promptly (would require many observations over a long time interval).

Conclusions. – We have simulated thermal evolution of a neutron star with a variable heater which is placed in a spherically symmetrical layer in the star's crust. Initially, the heater (whose nature is not specified) is assumed to be static and drives the star to a static state. Then we have varied (increased or decreased) the heater's power $L_h^\infty(t)$ over some time Δt and returned the heater to its initial steady state afterwards. The heater produces variations of the thermal surface luminosity $L_s^\infty(t)$; the main problem is if they are observable.

We have identified three main heat propagation regimes. The first is the dynamical regime when variations of $L_s^\infty(t)$ are almost independent of Δt, being governed by the thermal diffusion time t_{diff}. The second is the quasi-stationary regime in which the variations of $L_s^\infty(t)$ resemble those of $L_h^\infty(t)$ being mostly determined by Δt (rather than by t_{diff}). The third is the regime of fast neutrino cooling of the heater in a hot star when variations of $L_s^\infty(t)$ are strongly damped (almost invisible).

Our main result is that the observability of heater's variations is rather restricted – neutron stars are trying to hide their internal activity. To observe this activity, the heater and its variations have to be strong, but not too strong to avoid efficient neutrino cooling in the heater itself. Then the heater has to be rather close to the surface (placed at densities $\rho \sim 10^{11}$ g cm^{-3} or lower) to simplify heat transport to the surface. The heater's variation time Δt cannot be too short to produce enough variable heat energy but it cannot be very long to be detectable. Our results agree with the previous consideration [8] but seem more systematic (include studies of dips and of quasi-stationary regime).

The results obtained in the present work can be used for interpretation of observed variations of thermal radiation from neutron stars, particularly, from magnetars [4], and transiently accreting neutron stars in compact low-mass X-ray binaries [3,5].

The ability of neutron stars to greatly damp the effects of variable internal heaters on the surface emission does not mean that such effects are not observable at all. For instance, for very strong energy releases, with $H_0/H_c \gg 10$, the relative peak of the surface luminosity $L^\infty_{max}/L^\infty_c$ can be observable even for short energy releases, $\Delta t \gtrsim 1$ yr, provided the star is not very warm (H_c and L^∞_c are rather small). Our extra calculations for energy releases show that at each H_0/H_c-ratio there exists an optimal pre-burst amplitude H_c which provides maximum $L^\infty_{max}/L^\infty_c$ ratio, that depends on Δt. The higher H_0/H_c, the lower the optimal amplitude H_c. For instance, at $H_0/H_c \sim 3\times 10^3$ the optimal amplitude H_c decreases down to 10^{17}–10^{16} erg s^{-1}cm^{-3}.

Therefore, it is possible to obtain an enhancement of the peak of the surface luminosity by more than one or two orders of magnitude with relaxation tails continuing $\gtrsim 1$ yr, typical for the magnetar outbursts [13]. In this case the heater should produce a very large amount of energy ($H_0/H_c \gtrsim 10^3$) at a low pre-burst amplitude H_c. In particular, we confirm the possibility of a strong peak of the surface luminosity $L^\infty_{max}/L^\infty_c \sim 10^2$ with a relaxation tail lasting $\lesssim 10$ yr [14] in accordance with the observations of long outbursts of the central compact X-ray source 1E 161348–5055 in the SNR RCW 103 [15,16].

On the other hand, many magnetar outbursts are sufficiently strong and short. It would be difficult to explain them within the internal heater model unless the heater is placed uncomfortably close to the neutron star surface. This is an indirect argument in favor of widely discussed hypothesis that the radiation in such outbursts is formed in magnetospheres of magnetars [17].

Our results can be extended by considering a variety of neutron star models (different equations of state and stellar masses, and different models for nucleon superfluidity inside the stars), non-spherical heaters, different models for variability of the heaters; it would also be very important to include the effects of strong magnetic fields. Such extensions are certainly beyond the scope of this work. We expect that our main result (that internal heat variations are visible from the surface only under restricted conditions) will remain true in more extended studies.

* * *

The work was supported by the Russian Science Foundation, grant 14-12-00316.

REFERENCES

[1] Shapiro S. L. and Teukolsky S. A., *Black holes, white dwarfs, and neutron stars: The physics of compact objects* (Wiley-Interscience, New York) 1983.
[2] Haensel P., Potekhin A. Y. and Yakovlev D. G., *Neutron Stars. 1. Equation of State and Structure* (Springer, New York) 2007.
[3] Wijnands R., Degenaar N. and Page D., *MNRAS*, **432** (2013) 2366.
[4] Beloborodov A. M. and Li X., *ArXiv e-prints*, (2016) .

[5] Cumming A., Brown E. F., Fattoyev F. J., Horowitz C. J., Page D. and Reddy S., *ArXiv e-prints*, (2016) .
[6] Kaminker A. D., Potekhin A. Y., Yakovlev D. G. and Chabrier G., *MNRAS*, **395** (2009) 2257.
[7] Kaminker A. D., Kaurov A. A., Potekhin A. Y. and Yakovlev D. G., *MNRAS*, **442** (2014) 3484.
[8] Pons J. A. and Rea N., *Astrophys. J.*, **750** (2012) L6.
[9] Gnedin O. Y., Yakovlev D. G. and Potekhin A. Y., *MNRAS*, **324** (2001) 725.
[10] Potekhin A. Y., Chabrier G. and Yakovlev D. G., *Astron. Astrophys.*, **323** (1997) 415.
[11] Beznogov M. V., Potekhin A. Y. and Yakovlev D. G., *MNRAS*, **459** (2016) 1569.
[12] Potekhin A. Y., Fantina A. F., Chamel N., Pearson J. M. and Goriely S., *Astron. Astrophys.*, **560** (2013) A48.
[13] Coti Zelati F., Rea N., Papitto A., Viganò D., Pons J. A., Turolla R., Esposito P., Haggard D., Baganoff F. K., Ponti G., Israel G. L., Campana S., Torres D. F., Tiengo A., Mereghetti S., Perna R., Zane S., Mignani R. P., Possenti A. and Stella L., *MNRAS*, **449** (2015) 2685.
[14] Popov S. B., Kaurov A. A. and Kaminker A. D., *PASA*, **32** (2015) e018.
[15] De Luca A., Caraveo P. A., Mereghetti S., Tiengo A. and Bignami G. F., *Science*, **313** (2006) 814.
[16] De Luca A., Mignani R. P., Zaggia S., Beccari G., Mereghetti S., Caraveo P. A. and Bignami G. F., *Astrophys. J.*, **682** (2008) 1185.
[17] Beloborodov A. M., *Astrophys. J.*, **762** (2013) 13.